COSMOS, Vol. 9, No. 1 (2013) 1−10

DOI: 10.1142/S0219607713500055

FAST ION BEAM MICROSCOPY OF WHOLE CELLS

FRANK WATT*, CHEN XIAO*, CHEN CE-BELLE*,
CHAMMIKA NB UDALAGAMA*, REN MINQIN*,
G PASTORIN*,† and ANDREW BETTIOL*

*Centre for Ion Beam Applications
Department of Physics
National University of Singapore, Singapore 117542

†Department of Pharmacy
National University of Singapore

Received 14 September 2012
Revised 10 January 2013
Accepted 14 January 2013
Published 26 August 2013

The way in which biological cells function is of prime importance, and the determination of such knowledge is highly dependent on probes that can extract information from within the cell. Probing deep inside the cell at high resolutions however is not easy: optical microscopy is limited by fundamental diffraction limits, electron microscopy is not able to maintain spatial resolutions inside a whole cell without slicing the cell into thin sections, and many other new and novel high resolution techniques such as atomic force microscopy (AFM) and near field scanning optical microscopy (NSOM) are essentially surface probes. In this paper we show that microscopy using fast ions has the potential to extract information from inside whole cells in a unique way. This novel fast ion probe utilises the unique characteristic of MeV ion beams, which is the ability to pass through a whole cell while maintaining high spatial resolutions.

This paper first addresses the fundamental difference between several types of charged particle probes, more specifically focused beams of electrons and fast ions, as they penetrate organic material. Simulations show that whereas electrons scatter as they penetrate the sample, ions travel in a straight path and therefore maintain spatial resolutions. Also described is a preliminary experiment in which a whole cell is scanned using a low energy (45 keV) helium ion microscope, and the results compared to images obtained using a focused beam of fast (1.2 MeV) helium ions. The results demonstrate the complementarity between imaging using low energy ions, which essentially produce a high resolution image of the cell surface, and high energy ions, which produce an image of the cell interior. The characteristics of the fast ion probe appear to be ideally suited for imaging gold nanoparticles in whole cells. Using scanning transmission ion microscopy (STIM) to image the cell interior, forward scattering transmission ion microscopy (FSTIM) to improve the contrast of the gold nanoparticles, and Rutherford Backscattering Spectrometry (RBS) to determine the depth of the gold nanoparticles in the cell, a 3D visualization of the nanoparticles within the cell can be constructed. Finally a new technique, proton induced fluorescence (PIF), is tested on a cell stained with DAPI, a cell-nucleic acid stain that exhibits a 20-fold increase in fluorescence when binding to DNA. The results indicate that the technique of PIF, although still

at an early stage of development, has high potential since there does not seem to be any physical barrier to develop simultaneous structural and fluorescence imaging at sub 10 nm resolutions.

Keywords: Fast ion microscopy; whole cell imaging; proton induced fluorescence; gold nanoparticle imaging.

1. Introduction

Although focused nuclear particle beams have been around for several decades, both the development of the technology and the associated application areas are still some way from maturity. The prime distinguishing property of the nuclear particle probe, by which we mean a focused beam of fast nuclear particles e.g. MeV protons (hydrogen nuclei) or alpha particles (helium nuclei), is in the way this type of probe interacts with matter. The fast nuclear particle (ion) as it penetrates matter will mainly undergo collisions with atomic electrons, and for each collision only a small fraction of the ion energy is lost. In addition, as a consequence of the large mass difference between the ion and the atomic electron, ion/electron collisions do not result in significant deflection of the ion, and therefore the ion essentially travels in a straight line. After multiple electron collisions the nuclear particle slows down, and at the end of range the collision mechanism changes from electronic to predominantly nuclear collisions. In this end-of-range phase, the energy loss per collision is much higher, and any resultant deflections of the nuclear particle are significant. The primary property of a focused nuclear particle probe therefore is to travel in a straight line until the end of range, at which point there is an increase in the energy loss and a resultant spread of the beam.

Electron beam technology (e.g. electron microscopy, electron spectroscopy and electron lithography) is well developed, and the corresponding application areas are widespread. Electrons are low mass particles compared for example with a proton (by a factor of almost 2000), and as such do not penetrate into matter in the same way as fast ions. If the sample is thick enough, the primary electron will undergo collisions with atomic electrons, and suffer large energy loss and significant deflections with each collision. Although an electron beam can be focused to very small spot sizes (sub nm) at the surface of a sample, an electron beam in general does not travel in a straight line when interacting with matter and therefore is not as effective as a high resolution probe below the sample surface.

In the Centre for Ion Beam Applications, Dept of Physics, National University of Singapore, we can now focus an MeV nuclear particle beam (both protons and alpha particles) to spot sizes around 20 nm,[1,2] and the resulting resolution is much better than that can be achieved using conventional light microscopy ($\approx$250 nm). Because of this technological advance, we expect a rapid increase in the number of application areas which will benefit from the development of this new type of sub-surface probe, and one such application being pursued at the Centre for Ion Beam Applications is that of individual whole cell imaging. In addition there are many interesting techniques associated with a fast ion interacting with matter. Figure 1 outlines some of these interactions, and Table 1 lists the main characteristics of the associated techniques.

In this paper, we describe the way in which four of these techniques 'STIM, FSTIM, RBS and PIF' can be used to good effect for the high resolution imaging of whole cells.

2. Electron and Fast Ion Interactions with Organic Material

The focusing technology associated with the production of MeV nuclear particle probes is in general more complex than that for focusing keV electrons. It is therefore important that nuclear probes have significant advantages over existing electron probe techniques, otherwise further development will prove

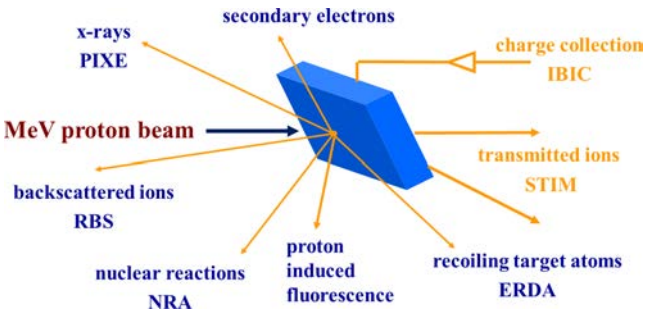

Fig. 1. Interaction of fast ion beams (e.g. MeV proton) with matter, and their associated techniques.

Table 1. Techniques available from the interaction between fast (MeV) ions and matter.

Associated technique	Technique characteristics
PISE — Proton Induced Secondary Electrons	As the ion beam penetrates into the sample, electrons are released from the surface. The secondary electrons can be collected to form an image of the surface topography.
PIXE — Particle Induced X-ray Emission	When the ion penetrating into the sample collides with atomic electrons this may result in a rearrangement of the inner shell electronic structure of the sample atom. Characteristic X-ray photons may be released from these excited atoms as they return to their ground state, and these photons can then be detected to produce quantitative elemental images of the sample down to the parts per million level.
RBS — Rutherford Backscattering Spectrometry	Although most ion collision events with the sample are electronic, there is a small probability that the incoming ion will interact with an atomic nucleus. If this collision results in the ion rebounding from the nucleus such that the ion backscatters out of the sample, then the sample elemental constituents and their depth within the sample can be assessed.
NRA — Nuclear Reaction Analysis	If the energy of the ion is higher than the coulomb barrier surrounding the nucleus, then the proton can be absorbed within the nucleus, and nuclear reactions can take place. NRA can be used for specific elemental and isotopic depth profiling.
PIF — Proton Induced Fluorescence	As a result of ion/electron collisions, the path of the ion beam through the sample is accompanied by the production of many short range secondary electrons. These secondary electrons can induce excited states in nearby atoms, resulting in de-excitation and a release of photons in the optical region of the electromagnetic spectrum. This process is similar, but not identical to, optical fluorescence microscopy.
ERDA — Elastic Recoil Detection Analysis	When heavy nuclear particles are used as the probe (e.g. MeV oxygen ions), there is a significant probability that lower mass surface atoms such as hydrogen are knocked out of the sample. By detecting the knock-out ions, ERDA can be used to provide an accurate estimate of low mass constituents in the sample.
IBIC — Ion Beam Induced Charge	If the sample is a semiconductor, then as the ion passes through the sample, it will induce electron−hole pairs which can be collected to give important information on the sample characteristics.
STIM — Scanning Transmission Ion Microscopy	STIM: If the sample is sufficiently thin so that the nuclear particles pass through and can be detected on the reverse side, then the energy loss of the transmitted ion can be used to provide important information on the localized electron density of the sample. If the transmitted ion is detected on axis, i.e. detected without any significant path deflection within the sample, then the energy loss is primarily derived from electronic collisions: STIM can be used for structural imaging.
FSTIM — Forward Scattering Transmission Ion Microscopy	FSTIM: If the transmitted ion is measured off axis, i.e. there has been significant deviation in the beam trajectory, then the ion has suffered both electronic and nuclear collisions. This technique can be used to increase the imaging contrast of heavy elements in a light matrix, since small angle deflections from nuclear scattering is much more probable for high Z elements.
	In general, fast ions such as MeV protons and MeV alpha particles are capable of passing through a whole cell.

redundant. In the Centre for Ion beam Applciations (CIBA), Department of Physics, NUS, we have developed a Monte-Carlo simulation software package in order to simulate the trajectories of primary charged particles (e.g. electrons or ions) in matter and also to determine their energy deposition profiles.[3] This software package, DEEP — Deposition of Energy due to Electrons and Protons — extends the standard simulation model for ion beam tracking SRIM,[4] by incorporating EEDL97 data[5] and volume plasmon localization and electron generation models (Hansen-Kocbach-Stolterfoht).[6]

Figure 2 demonstrates the prime advantage of using a focused beam of 1 MeV protons compared with 25 keV electrons. The simulations are for the primary particle beams focused to a point and

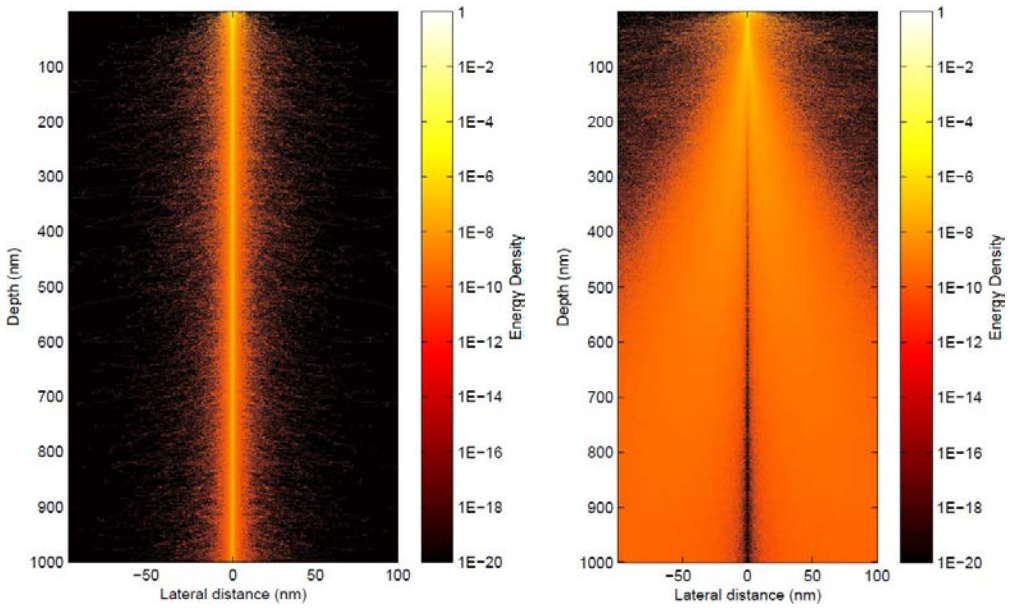

(a) (b)

Fig. 2. Energy deposition of (a) 1 MeV proton beam and (b) focused 25 keV electron beam penetrating the top 1 micron of organic material (PMMA). Simulations using the DEEP software package.[3]

subsequently penetrating the top 1 micron of Polymethyl methacrylate (PMMA), a common organic material. As can be observed, the trajectories and lateral energy deposition for the 25 keV electrons increases rapidly as the electron beam penetrates the PMMA, reaching ±100 nm at a depth of around 400 nm. The proton beam on the other hand retains its straight trajectory, with very little energy deposition outside a diameter of 10 nm from the primary proton track. Similar results are observed when other energies (10 keV−1 MeV for electrons, and 0.5−3 MeV for protons and helium ions) are considered.[7]

These simulations confirm the expected difference in properties of focused electrons and ions, and indicate that whilst focused electron beams are extremely useful for imaging surface structure and determining surface properties, they are inferior to fast ions when probing the sub-surface regions of relatively thick specimens at high resolutions.

3. Whole Cell Imaging Using Slow and Fast Ions

Optical microscopy has a fundamental limit imposed on the spatial resolutions that can be achieved due to the effects of diffraction, and as such there has been a rapid push towards new techniques that can break this diffraction limit. The quest for high resolution optical microscope technologies has led to the development of super-resolution optical imaging techniques, including Photo-Activated Localization Microscopy (PALM and FPALM),[7,8] Stochastic Optical Reconstruction Microscopy (STORM),[9,10] Stimulated Emission Depletion (STED)[11] and Saturated Structured-Illumination Microscopy (SSIM).[12] These new optical techniques, which have their own advantages and limitations, are capable of breaking the optical diffraction limit and are being used in the study of cellular ultrastructure.

In work carried out recently,[13] we have attempted a comparative investigation into whole cell microscopy using fast and slow ions. Slow (e.g. 10−50 keV) helium ion beams can now be focused to sub-nanometre dimensions (∼0.25 nm) using the Zeiss Helium Ion Microscope. However, because keV helium ions lack the penetrating power to pass through a whole cell, this type of microscopy is limited to imaging the surfaces of cells at high resolutions through the detection of induced secondary electrons. Interestingly, because of the high mass of the helium ion coupled with the ease of neutralizing the sample charging using a flood electron beam, surface charging effects are minimal. Cell surfaces can therefore be imaged without the need for a conducting metallic coating, a procedure necessary in electron microscopy for insulating samples such as whole cells. Fast (MeV) helium ions on the other

hand have the penetrating power to pass through a whole cell, as well as maintaining a straight path. Along the ion trajectory the fast helium ion undergoes multiple electron collisions and for each collision a small amount of energy is lost to the scattered electron. Nuclear collisions are relatively rare and large angle scattering is minimal. By measuring the total energy loss of each MeV helium ion as it passes through the cell, an energy loss image can be assembled which is representative of the mass distribution of the cell (Scanning Transmission Ion Microscopy—STIM).

The cells chosen for this comparative study were human fetal liver cells.[14] The cells were seeded on to silicon nitride windows of thickness 100 nm at a density of 10 000 cells/cm^2 and allowed to attach for 24 hrs prior to fixation in 4% formaldehyde. Samples were then dehydrated through an ethanol gradient followed by critical point drying[15] before scanning the sample in the MeV ion cell imaging facility at the Centre for Ion Beam Applications, Department of Physics, National University of Singapore. A beam of 1.2 MeV helium ions was focused into a spot size of around 40 nm, and scanned over the sample. Each transmitted ion was detected using a surface barrier silicon particle detector placed behind the sample, and by using list mode event-by-event data acquisition procedures, scanning transmission energy loss data from each ion were assembled into 1024×1024 pixel arrays as STIM images. PIXEL normalization was utilized in order to reduce statistical noise: at each pixel exactly 15 ions were detected and their energies recorded. The median energy of these 15 ions was used to construct the final image. Figure 3 shows the results of this comparison: Figure 3(a) shows a helium ion microscope

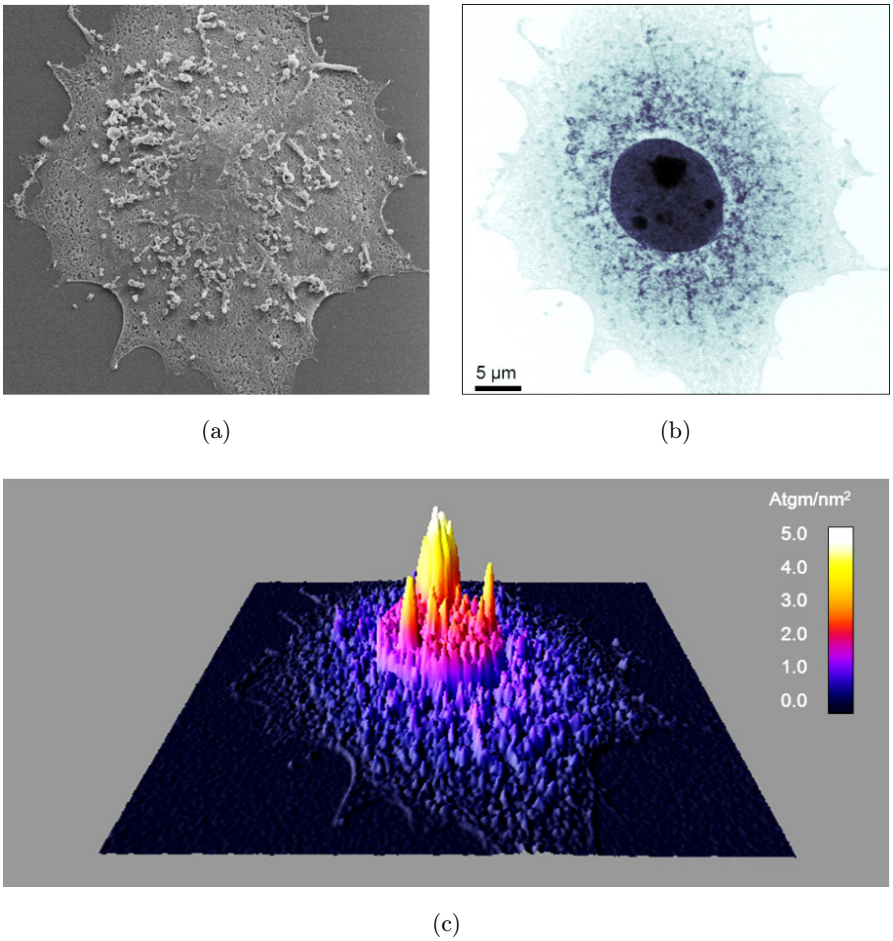

(a) (b)

(c)

Fig. 3. (a) Helium ion microscope image of a human liver cell, showing surface features. Helium ion energy = 45 keV, (b) Helium ion transmission energy loss images of the same cell, showing structural features common to the surface as well as structural features from within the cell. Helium ion energy = 1.2 MeV and (c) Mass image showing a 3D plot of the mass distribution (in units atto-gram/nm^2): [1 attogram = 10^{-18} gms]: Helium ion energy = 1.2 MeV. Figures reproduced from Ref. 13.

image of a whole cell plated on to the silicon nitride window, Fig. 3(b) shows a STIM image of the same cell, and Fig. 3c shows a mass distribution image. These images represent how helium ion microscopy at two different energies can provide complementary information: slow ions provide an image of the cell surface at high resolution, and fast ion imaging provides structural information from the cell interior, including the nucleus, nucleoli, and what are possibly internal organelles of unknown origin. Interestingly, Fig. 3(c) indicates that the densities of the observed nucleoli appear much higher than the average density of the nucleus, which in turn is much higher than the cytoplasm density and constituent structures. It must be emphasized that when MeV ions are used, then the resolution (in this case 40 nm) is maintained throughout the cell. As far as we know, there is no comparative technique that can achieve this type of structural data with this resolution and contrast.

4. Detection of Gold Nanoparticles Inside a Whole Cell

One avenue of exploration that may benefit from the ability to image the interior of whole cells at high resolution is that of investigations into nanoparticle (NP) uptake and redistribution within whole cells. This is important since nanoparticles may be useful in the future as potential drug delivery systems (DDS).[16] NPs have reduced dimensions and hence have the ability to penetrate cell membranes without compromising the cell integrity. NPs can also undergo surface functionalization to include targeting and delivery molecules. Clearly, any advanced microscopy that allows high resolution imaging of nanoparticles in whole cells would represent an important step forward.

We have investigated the use of fast ion microscopy to locate gold NanoParticles (AuNPs) within a whole cell.[17] The cell samples were prepared as follows: HeLa cells were seeded on to silicon nitride windows of thickness 100 nm at a density of 6000 cells/cm^2 in Dulbecco's modified Eagle's medium (DMEM) supplemented with FBS (10%) and antibiotics penicillin (100 units/ml) and streptomycin (100 μg/ml). After cell attachment, control cells were rinsed with PBS and incubated in supplemented DMEM. The test (NP) cells were similarly incubated but also exposed to FBS-coated 100 nm AuNPs (5 pM) for 24 hrs. Both control and NP cells were washed three times with prewarmed PBS and fixed in gluteraldehyde (2.5%) for 24 hrs. Fixed cells were then dehydrated using an ethanol gradient before critical point drying.

Figure 4(a) shows an electron micrograph of the surface of one of the AuNP cells: evidence of both single and clustered AuNPs are observed on the surface of the cell and on the silicon nitride window around the cell. The control cell (not shown), as expected, did not exhibit any AuNPs either on the surface or in the area surrounding the cell. The STIM image of the same AuNP cell is observed in Fig. 4(b), and although there is evidence of AuNPs associated with the cell and the surrounding area, the contrast in the figure is masked by the high density associated with both the nucleus and regions of the cytoplasm. Figure 4(c) is a higher magnification scan over the cell, and shows the NPs with a slightly better contrast. However, it is still difficult from this image to distinguish gold nanoparticles from other structures of the same size associated with the cell. In addition, it is difficult to distinguish the AuNPs on the surface of the cell with those that have been ingested into the cell interior.

In order to increase the image contrast for the gold nanoparticles, we can use the technique of FSTIM. There is a reduced probability that the incoming fast ions interact with the nuclei of the atoms in the cell. For such cases the angle through which the incident ions are scattered is given by the well-known formula

$$\sigma = \left[\frac{Z_1 Z_2 e^2}{4E_c \sin^2(\theta_c/2)}\right]^2,$$

where σ is the cross section (probability) for nuclear elastic collisions, Z_1 is the atomic number of the incoming ion, Z_2 is the atomic number of the target nucleus, E_c is the incoming ion energy, and θ_c is the scattering angle from the original ion path.

If we use the above equation to compare the scattering of primary ions from gold atoms ($Z = 79$) and carbon atoms ($Z = 6$) we can observe a ratio of $(79/6)^2 \approx 173$ increase in scattering probability. The increase in scattering results in a significant increase in contrast for the gold nanoparticles compared with the normal constituents of organic tissue. This increase in contrast can be observed in Fig. 4(d), where the gold nanoparticles (both individual and in clusters) can be clearly observed.

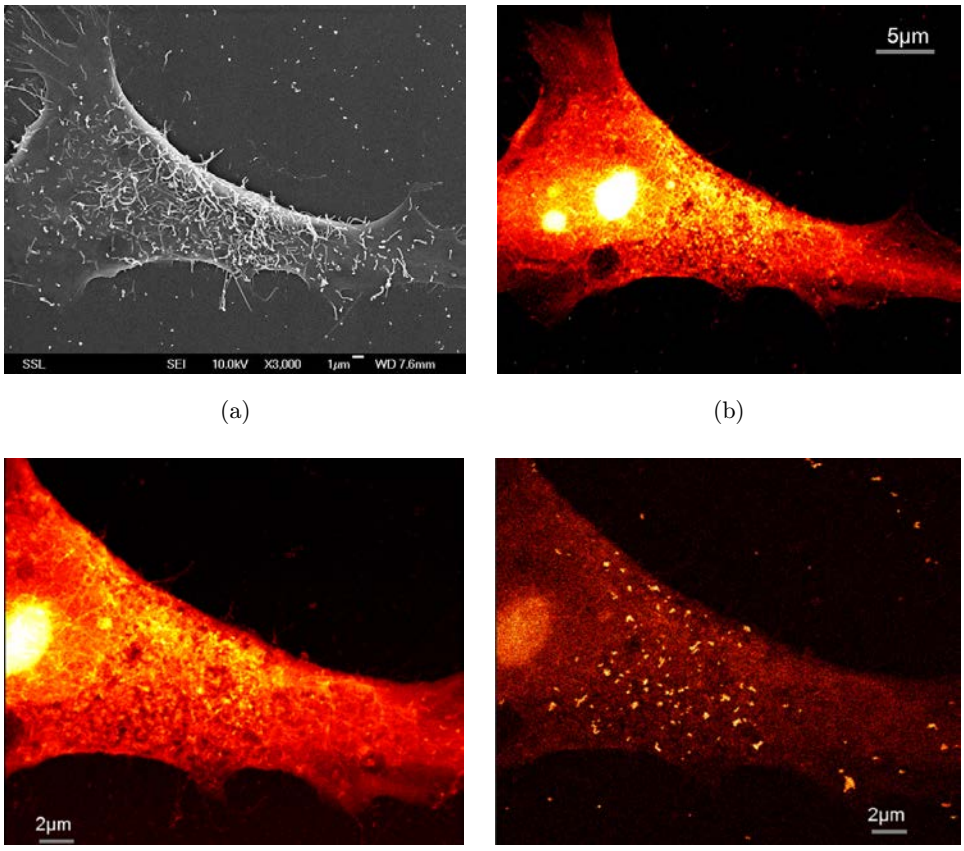

Fig. 4. (a) Scanning electron micrograph of a HeLa cell cultured in an environment of AuNPs, (b) Alpha particle STIM image of the same Hela cell cultured in an environment of AuNPs, (c) Higher magnification scanning transmission ion microscopy (STIM) images of the AuNP HeLa cell and (d) FSTIM image of the HeLa cell showing high contrast for the AuNPs. [All images taken using 1.6 MeV helium ions]. Figures reproduced from Ref. 17.

The final step is to distinguish the AuNPs which are present on the surface of the sample from the NPs that have been incorporated into the cell, presumably through the process of endocytosis. For this we can use the well-known technique of Rutherford Backscattering Spectrometry (RBS). If we measure the energy of incident ions that rebound at a backward angle from the target atom nuclei, then the depth of each individual AuNP or AuNP clusters in the cell can be determined. Figure 5 shows the results of depth determination for the AuNPs. The number of AuNPs can also be assessed quantitatively using the ion scattering techniques of RBS and FSTIM. For the cell shown in Figs. 4 and 5, it can be determined that 1341 gold NPs (including those in clusters) have been internalized by the cell.

It can be anticipated that this combination of techniques can be used to elucidate the mechanisms

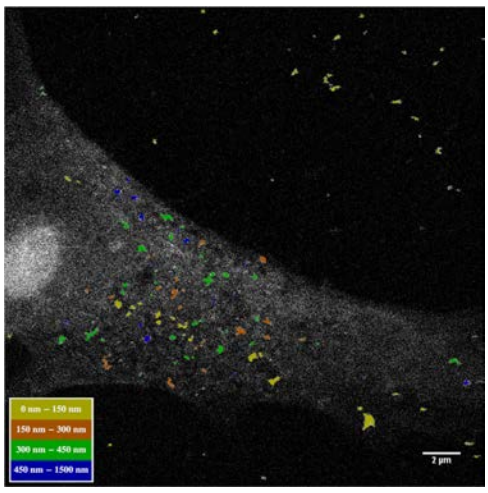

Fig. 5. AuNP depth distribution in the HeLa cell as shown in Fig. 4: Rutherford backscattering data, color coded to give depth information. Figure reproduced from Ref. 17.

of endocytosis and track functionalized gold nanoparticles into targeted areas of the cell at spatial resolutions around 20 nm.

5. High Resolution Proton Induced Fluorescence (PIF)

Because a beam of MeV protons is able to travel through a whole cell without much deviation in trajectory, the spatial resolution of this type of probe is maintained in STIM images. However, as we can observe in Fig. 2, there is a cylindrical 'halo' of secondary electrons associated with the primary particle beam which deposits energy laterally from the proton path. This halo however does not extend very far and, depending on the proton energy, is normally contained within 5 nm of the primary particle track. The secondary electron halo can excite nearby atoms into excited states, which can de-excite by emitting optical photons. Up to now, this process of proton induced fluorescence (PIF) has not been explored using biological systems, apart from a few preliminary tests.[18–20] However, the future potential of PIF as applied to whole cells is extremely good, since the resolution achievable for PIF is only slightly greater than the proton spot size, and since this is currently around 20 nm, this already exceeds the resolution of conventional fluorescence microscopy by an order of magnitude. In addition, simultaneous structural images are achievable, making this a unique combination of techniques.

Figure 6 shows a preliminary test of PIF using MRC5 — human fetal lung fibroblast cells grown on 100 nm silicon nitride windows and stained with DAPI, a nucleic acid stain that exhibits a 20-fold increase in fluorescence upon DNA binding. Figure 6(a) shows a 1 MeV proton STIM image of a single cell, and Fig. 6(b) demonstrates the effectiveness of proton induced fluorescence imaging. In this test, the spatial resolution of the STIM image was estimated at 30 nm, and the PIF image estimated at 80 nm. It must be recognized that for this test the collection efficiency of the fluorescence signal has not been optimised, and hence image quality is not ideal. Nevertheless, whilst the results of this particular preliminary test do not represent a significant leap forward in resolution with respect to optical fluorescence imaging, it does however indicate its potential in that there is no physical reason why simultaneous structural and fluorescence imaging should not be possible at resolutions much higher than presently attainable.

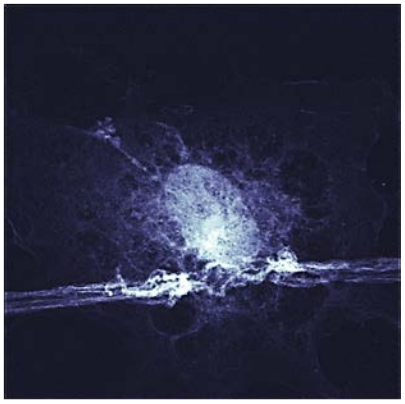

(a)

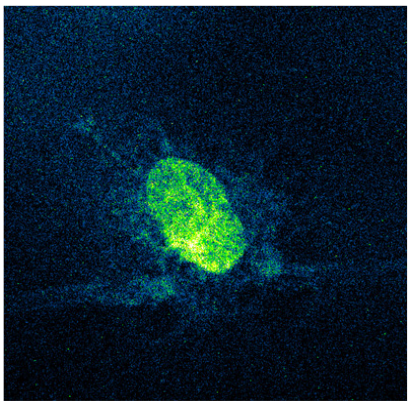

(b)

Fig. 6. (a) Proton STIM image of a MRC5 human fetal lung fibroblast cell: Proton energy 1 MeV, substrate 100 nm silicon nitride film and (b) Proton Induced Fluorescence (PIF) image of the same cell: Proton energy 1 MeV. PIF images taken using a miniature Hamamatsu R7400m photomuliplier tube.

6. Conclusions

The ability of fast (MeV) ions, e.g. protons and helium ions (alpha particles), to penetrate several microns of organic tissue (e.g. whole cells) whilst maintaining an almost straight path, gives us an important probe to investigate the interior of biological cells.

One specific example is described, that of using a focused beam of MeV alpha particles to visualize and quantify the 3D internalization of gold nanoparticles in a HeLa cell, using a combination of STIM, FSTIM and RBS. Currently we can visualize

the three dimensional location of gold NPs at lateral resolutions of ~ 25 nm and depth resolutions ~ 60 nm in whole cells. The imaging times are relatively fast, with STIM and FSTIM taking around 15 min per cell, and RBS imaging (used to ascertain the depth of the particles in the cell) taking around 1 hr. It can be envisaged that in the future, microscopy using MeV ions will enable a quantitative evaluation of particle accumulation in specific cellular organelles and provide useful insights into the mechanism of internalization and the intracellular bio-distribution of drugs. By visualizing the accumulation of nanoparticles, for example in correspondence with lysosomes which are organelles commonly involved in the digestion of molecules and particles deriving from phagocytosis, endocytosis and autophagy, we can perhaps elucidate the mechanism involved and discriminate between an energy-mediated (i.e. active transport) or energy-independent cellular nanoparticle up-take.

A second example, which essentially is still in the test phase, is that of utilizing the properties of the fast ion beam to induce fluorescence in the sample. This is analogous to inducing a fluorescence signal using a higher photon energy (e.g. optical fluorescence microscopy or confocal microscopy using lasers), except that in this case the excitation mechanism is from short range ion induced secondary electrons. The potential of this technique is still to be realized, but the promise of simultaneous structural and fluorescence imaging at the 10 nm level and below should not be underestimated.

References

1. Watt F, Chen X, de Vera AB, Udalagama CN, R Minqin, van Kan JA and Bettiol AA, The Singapore high resolution single cell imaging facility, *Nuclear Instruments & Methods in Physics Research B* **269**:2168−2174, 2011.
2. van Kan JA, Malar P and de Vera AB, The second generation Singapore high resolution proton beam writing facility, *Review of Scientific Instruments* **83**:02B902, 2012.
3. Udalagama C, Bettiol AA and Watt F, Stochastic spatial energy deposition profiles for MeV protons and keV electrons, *Phys Rev B* **80**:224107, 2009.
4. Ziegler JF and Biersack JP, The stopping and range of ions inmatter, SRIM software, http://www.srim.org/
5. Perkins ST and Cullen DE, Lawrence livermore national laboratory, Report No. UCRL-117796, 2002; http://wwwnds.iaea.org/epdl97; http://www.llnl.gov/cullen1
6. Hansen J and Kocbach L, *J Phys B* **22**:L71, 1989.
7. Betzig E *et al.*, Imaging intracellular fluorescent proteins at nanometer resolution, *Science* **313** (5793):1642−1645, 2006.
8. Hess ST *et al.*, Dynamic clustered distribution of hemagglutinin resolved at 40 nm in living cellmembranes discriminates between raft theories, *Proceedings of the National Academy of Sciences* **104** (44):17370−17375, 2007.
9. Huang B, Wang W, Bates M and Zhuang X, Three-Dimensional super-resolution imaging by stochastic optical reconstruction microscopy, *Science* **319**(5864):810−813, 2008.
10. Huang B, Jones SA, Brandenburg B and Zhuang X, Whole-cell 3D STORM reveals interactions between cellular structures with nanometer-scale resolution, *Nat Meth* **5**(12):1047−1052, 2008.
11. Willig KI, Rizzoli SO, Westphal V, Jahn R and Hell SW, STED microscopy reveals that synaptotagmin remains clustered after synaptic vesicle exocytosis, *Nature* **440**(7086):935−939, 2006.
12. Schermelleh L *et al.*, Subdiffraction multicolor imaging of the nuclear periphery with 3D structured illumination microscopy, *Science* **320**(5881): 1332−1336, 2008.
13. Chen X, CNB Udalagama, Chen C-B, Bettiol A, Pickard D, Venkatesan T and Watt F, Whole cell imaging using fast and slow helium ions, *Biophysical Journal* **101**:1788−1793, 2011.
14. Tan TMC, Sit KH and Wong KP, Kinetics of sulphate conjugation in extracts of human foetal liver cells in culture, *Biochem Pharmacol* **37**:4629−4633, 1988.
15. Minqin R, van Kan JA, Bettiol AA, Daina L, Gek CY, Huat BB, Whitlow HJ, Osipowicz T and Watt F, Nano-imaging of single cells using STIM, *Nuclear Instruments & Methods in Physics Research B* **260**:124−129, 2007.
16. Papasani MR, Wang G and Hill RA, Gold nanoparticles: The importance of physiological principles to devise strategies for targeted drug delivery, *Nanomedicine: Nanotechnology, Biology and Medicine* **8**(6):804−814, 2012.
17. Chen X, Chen C-B, Udalagama CNB, Ren M, Fong KE, Yung LYL, Giorgia P, Bettiol AA and Watt F, High resolution 3D imaging and quantification of gold nanoparticles in a whole cell; Nanomed (to be published).
18. Watt F, Bettiol AA, van Kan JA, Ynsa MD, Minqin R, Rajendran R, Huifang C, Sheu F-S, Jenner AM,

Imaging of single cells and tissue using MeV ions, *Nuclear Instruments and Methods in Physics Research B* **267**:2113−2116, 2009.

19. Pallon J, Yang C, Utui RJ, Elfman M, Malmqvist KG, Kristiansson P and Sjijland KA, *Nucl Instr Meth B* **130**:199, 1997.
20. Rossi P, Di Maggio C, Egeni GP, Galligioni A, Gennaro G, Giacomelli L, Lo Giudice A, Pegoraro M, Pescarini L, Rudello V and Vittone E, *Nucl Instr Meth B* **181**(1−4):437, 2001.